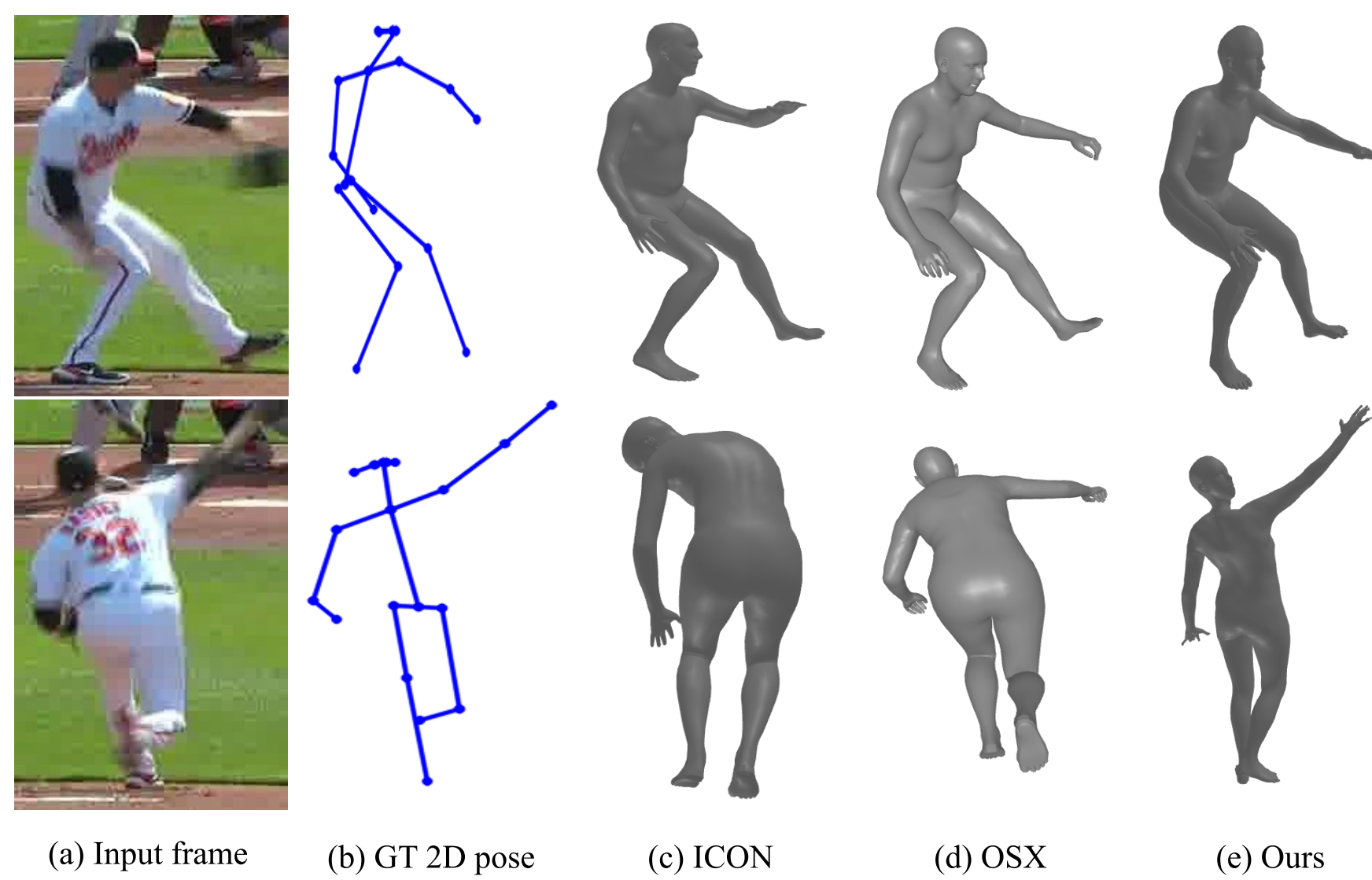


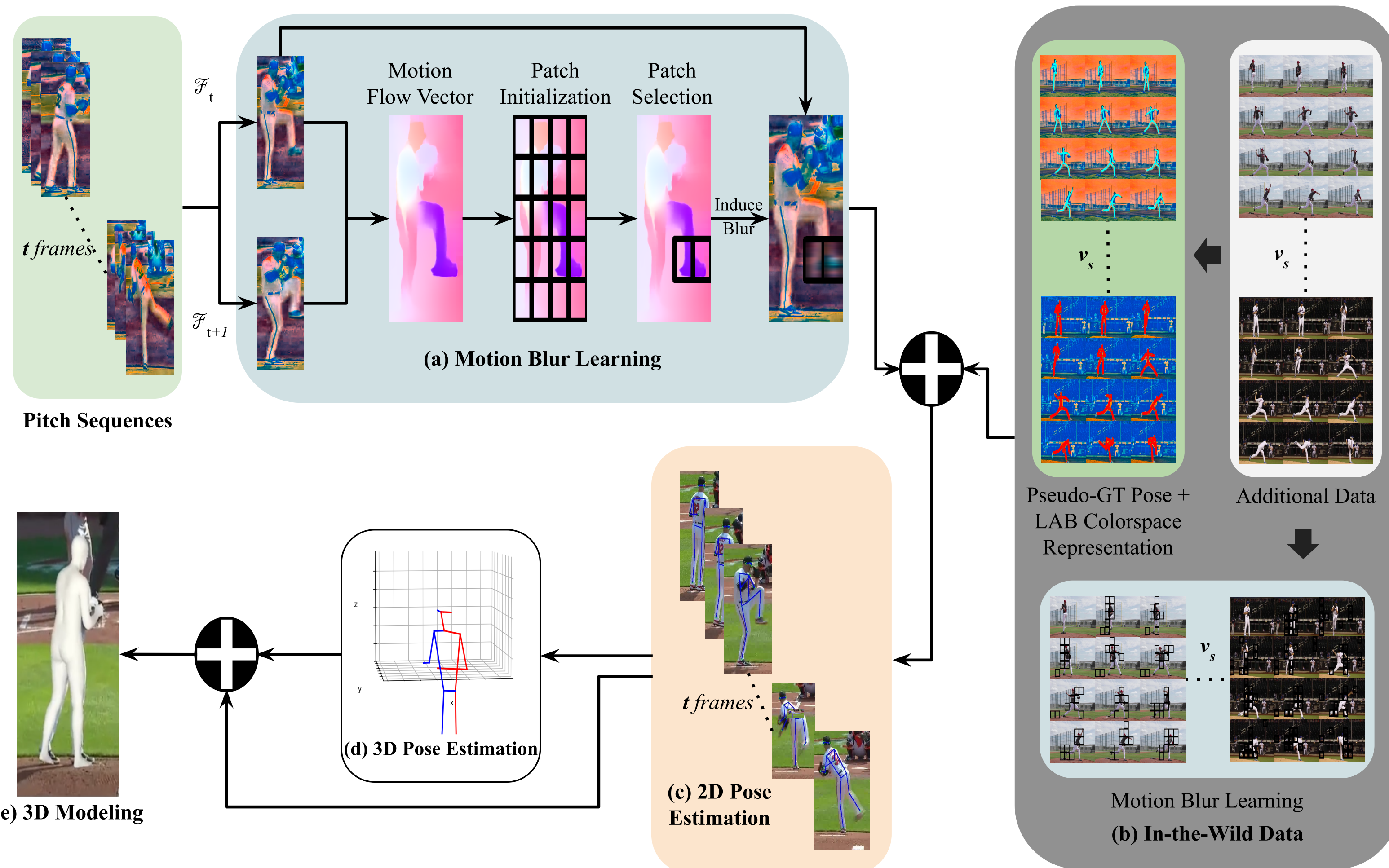
JERRIN BRIGHT, YUHAO CHEN AND JOHN ZELEK
UNIVERSITY OF WATERLOO, WATERLOO, ONTARIO, CANADA

KEY CONTRIBUTIONS

- A focused augmentation strategy incorporating motion blur artifacts, challenging conventional belief in pipelines.
- Leveraging in-the-wild datasets, aids in capturing the variability and complexity present in the data.
- Improved performance of existing pose estimators with proposed framework incorporation, where we demonstrate the substantial enhancement
- Spatiotemporal cost reinforced by histogram representations, to effectively align partially synchronized frames.



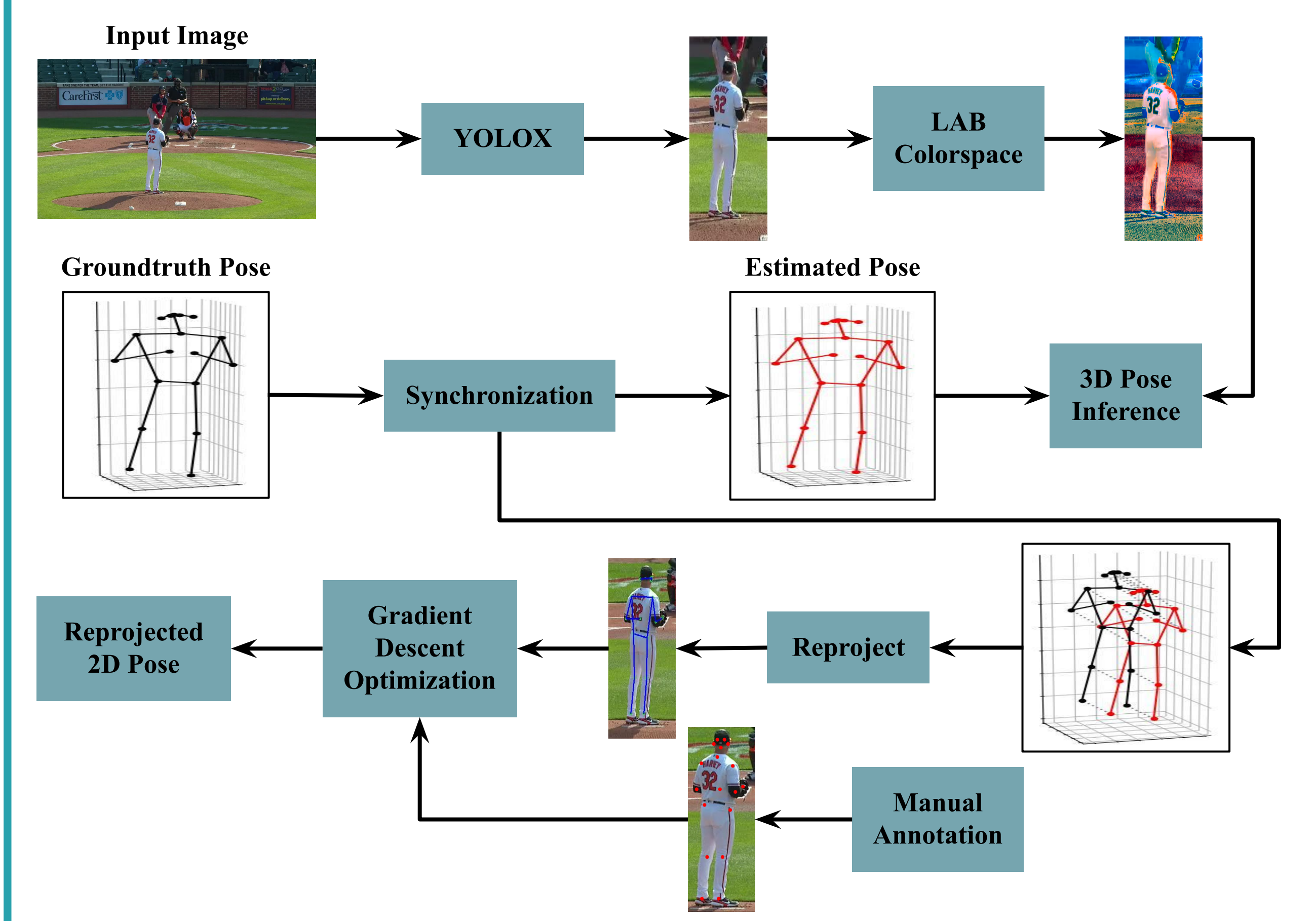
METHODOLOGY



The proposed approach comprises several key steps:

- Data Representation:** Each pitch sequence is represented as $\hat{\mathcal{P}} = \{\mathcal{F}_t : \mathcal{F}_t \in \mathbb{R}^{H \times W \times 3}\}_{t=1}^{t_n}$.
- Motion Blur Augmentation:** Motion flow (MF) between consecutive frames is analyzed by dividing each frame into k patches. The top N patches with the highest MF are selected as target regions for inducing blur.
- 2D Pose Estimation:** In each frame \mathcal{F}_t , the 2D pose of the pitcher is estimated, resulting in $\mathcal{P}_{2D}^{(t)} \in \mathbb{R}^{\mathcal{J} \times 2}$.
- 3D Pose Estimation:** Utilizing a receptive field of s consecutive 2D pose ($\mathcal{P}_{2D} \in \mathbb{R}^{s \times \mathcal{J} \times 2}$), the 3D pose of the pitcher is estimated, producing $\mathcal{P}_{3D} \in \mathbb{R}^{1 \times \mathcal{J} \times 3}$.
- Concatenation:** The 2D and 3D poses are concatenated represented by $\mathcal{P}_{\text{concat}}^{(t)} \in \mathbb{R}^{1 \times \mathcal{J} \times 5}$.
- Human Mesh Recovery:** The 3D body mesh represented by $\mathcal{H}_{3D} \in \mathbb{R}^{\mathcal{V} \times 3}$ is then modeled using spectral convolutional networks [1].

DATASET



Synchronization: Warping the time axis and minimizing the distance (cost) between the sequence. A one-to-one hard constraint was assigned with a weighted cost function (\mathcal{G}).

$$\mathcal{G} = g_s \left(\frac{1}{\mathcal{J}} \sum_{i=1}^{\mathcal{J}} (kp_{gt}^{(i)} - kp_{pred}^{(i)})^2 \right) + g_t \left(1 - \frac{\sum_{i=1}^{\mathcal{J}} kp_{gt}^{(i)} \cdot kp_{pred}^{(i)}}{\sqrt{\sum_{i=1}^{\mathcal{J}} (kp_{gt}^{(i)})^2} \cdot \sqrt{\sum_{i=1}^{\mathcal{J}} (kp_{pred}^{(i)})^2}} \right) \quad (1)$$

Camera Projection: Through a process of gradient descent optimization, we iteratively refine the initialized focal length (f_i), which will be used to reproject the 3D GT pose to 2D image coordinate.

$$\hat{f} = f_i - \alpha \Delta L(f_i) \quad (2)$$

ACKNOWLEDGEMENT

Our work was supported by the Baltimore Orioles, MLB through the Mitacs Accelerate Program. We also acknowledge the Digital Research Alliance of Canada for their hardware support.



REFERENCES

- Hongsuk Choi, Gyeongsik Moon, and Kyoung Mu Lee. Pose2mesh: Graph convolutional network for 3d human pose and mesh recovery from a 2d human pose. *ECCV 2020*, pages 769–787, 2020.
- Kaan Koseler and Matthew Stephan. Machine learning applications in baseball: A systematic literature review. *Applied Artificial Intelligence*, 31:1–19, 02 2018.

RESULTS

Performance of different SOTA 2D pose techniques.

| Method | Type | MB | Loss |
|------------------|------------|----|--------------|
| Xu et al | Heatmap | | 1.37 |
| Ke et al | Heatmap | | 1.46 |
| Panteleris et al | Regressor | | 1.15 |
| Li et al. | Heatmap | | 1.83 |
| Mao et al. | Regression | | 1.26 |
| Xu et al | Heatmap | ✓ | 1.17 (+0.20) |
| Ke et al | Heatmap | ✓ | 1.21 (+0.25) |
| Panteleris et al | Regressor | ✓ | 0.55 (+0.60) |
| Li et al. | Heatmap | ✓ | 1.46 (+0.37) |
| Mao et al. | Regressor | ✓ | 0.61 (+0.65) |

Results of the estimated pose with different modules.

| Base Model | ItW | MB | 2D Loss | 3D Loss |
|------------|-----|----|-------------|-------------|
| ✓ | | | 1.05 | 1.93 |
| ✓ | ✓ | | 0.88 | 1.61 |
| ✓ | | ✓ | 0.55 | 1.47 |
| ✓ | ✓ | ✓ | 0.48 | 1.23 |

Study on the region size and frequency of blur effect

| $s_{patch} \mathcal{N}$ | 1 | 3 | 5 | 7 | 9 |
|---------------------------|------|-------------|------|-------|------|
| 10 | 0.83 | 0.74 | 0.66 | 0.64 | 0.67 |
| 20 | 0.71 | 0.57 | 0.62 | 0.60 | 0.62 |
| 30 | 0.68 | 0.55 | 0.61 | 0.639 | 0.59 |
| 40 | 0.74 | 0.63 | 0.68 | 0.75 | 0.78 |

LOSS FUNCTIONS

The loss function leveraged for 2D and 3D pose estimators is the Euclidean distance between γ dimensions, defined as:

$$\mathcal{L}_{pose} = \frac{1}{\mathcal{N}} \sum_{i=1}^{\mathcal{N}} \frac{1}{\mathcal{J}} \sum_{j=1}^{\mathcal{J}} \|kp_{pred}^{(ij)} - kp_{gt}^{(ij)}\|_{\gamma} \quad (3)$$

where,

$$\|\cdot\|_{\gamma} = \begin{cases} \|\cdot\|_2, & \text{if } \gamma = 2 \text{ (for } \mathcal{P}_{2D}) \\ \|\cdot\|_3, & \text{if } \gamma = 3 \text{ (for } \mathcal{P}_{3D}) \end{cases}$$

The loss function employed for human mesh recovery encompasses vertex, joint, normal, and edge loss, defined as:

$$\mathcal{L}_{mesh} = \lambda_v \mathcal{L}_v + \lambda_j \mathcal{L}_j + \lambda_n \mathcal{L}_n + \lambda_e \mathcal{L}_e \quad (4)$$

CONCLUSION

- Innovative Augmentation for Motion Blur:** The research introduces a unique technique to strategically enhance motion blur, improving the network's ability to handle this challenge during pose estimation.
- In-the-Wild Video Data Integration:** Incorporating in-the-wild video data, along with pseudo-groundtruth pose information, improves the network's performance under varying lighting and camera conditions.
- Significant Accuracy Improvement:** Substantial increase in SOTA pose estimation accuracy, particularly during pitching actions, underscores the importance of thoughtful augmentation to address motion blur.